EVOLUTION OF THE EAST AFRICA-ARABIA PLUME HEAD

Chiara Civiero[1*], Sergei Lebedev[1], Nicolas L. Celli[1]

(1) Dublin Institute for Advanced Studies (DIAS), Geophysics Section, 5 Merrion Square, Dublin D02 Y006, Ireland

EGU General Assembly 2021
vEGU21: Gather Online

1. Introduction

Mantle plumes are thought to form large, round heads followed by thin tails. Volcanism in is distributed unevenly over up to thousands of km across. This would require unrealistically wide plume-head circles.

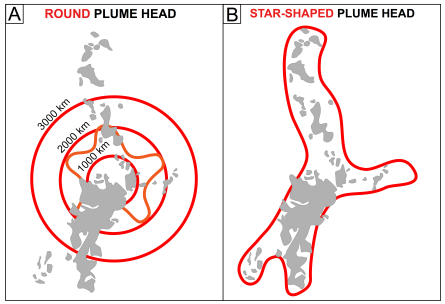


Figure 1. A) Classical round or fingered plume head. CB) More complex, star-shaped plume head below dispersed LIP volcanism.

2. East Africa-Arabia region

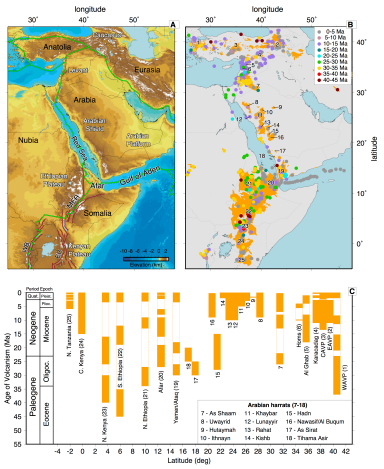


Figure 2. A) Topography of the region of study. B) Location of the volcanic rocks. C) Age-latitude plot of the igneous activity.

Active dispersed volcanism throughout the process of continental breakup and rifting.

Long standing puzzle on what causes rifting, diffuse volcanism, and uplift.

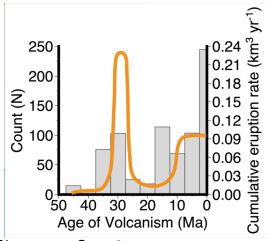


Figure 3. Spatio-temporal distribution of the volcanism (eruption rates and dated rocks).

3. Dataset

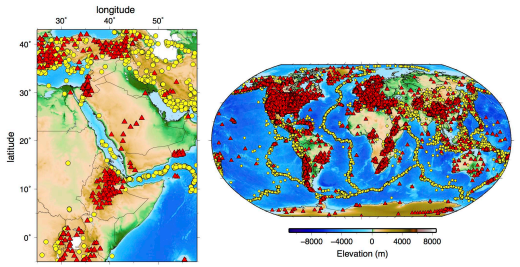
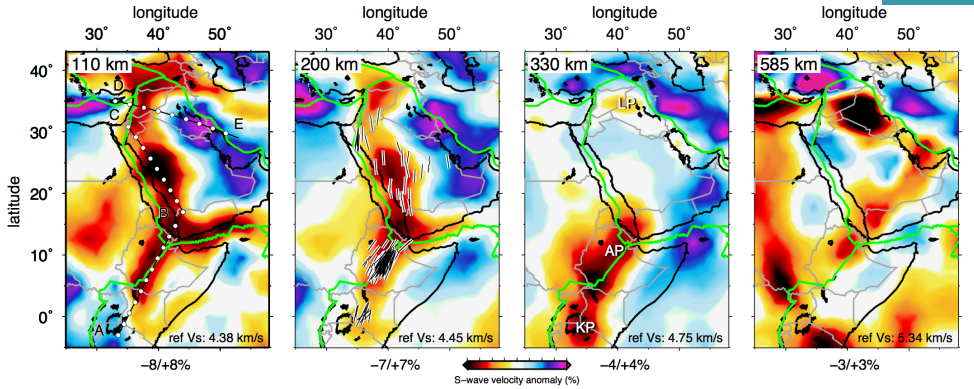


Figure 3. Earthquakes and seismic stations within the study area and around the globe. Events are plotted as yellow circles, seismic broadband stations as red triangles.

The azimuthally anisotropic, S-wave speed, tomographic model is constrained by over **1.2 million seismograms, waveform-fitted** using the Automated Multimode Inversion (AMI) of surface- and S-waveforms.

4. Shear-wave model



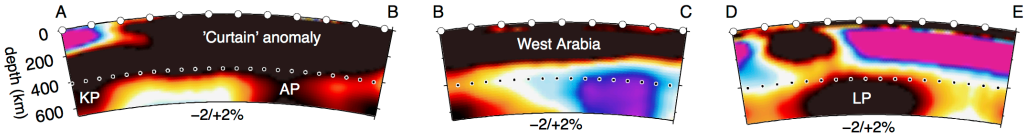


Figure 4. Top left panels: Depth slices of the S-wave model [*Celli et al., 2020*] at 110, 200, 330 and 585 km. The SKS splitting measurements [*Gao et al., 2010*] are plotted in the map view at 200 km depth. Right right panels: cross-sections through the main low-velocity features of the model.

Large, three-pointed star low-velocity anomaly centered in Afar and composed of three branches:

- Curtain-like anomaly in the upper mantle below East Africa connecting Kenya and Afar Plumes.
- Low-velocity channel underlying West Arabia.
- Low-velocity anomaly following the Gulf of Aden rift.

Low-velocity anomaly extending though the transition zone below Levant region (Levant Plume).

5. Resolution tests

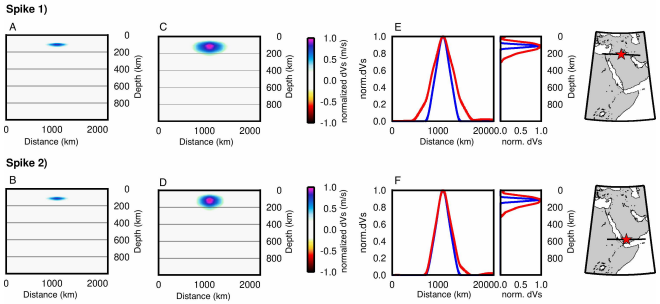


Figure 5. Synthetic spike test. A-B) Cross-sections of the two spikes at 110 km depth through the input model. C-D) Cross-sections through the output model. Orientation of the cross-section is shown on the maps in black. E-F) Vertical and horizontal 1D *S*-wave anomaly profiles along the cross-sections.

Good recovery of synthetic structures, particularly within the upper 300 km, with our dataset.

The spurious structure as seen in the output is small and cannot be responsible for the observed anomalies.

Our model is capable of resolving the low-velocity features reliably.

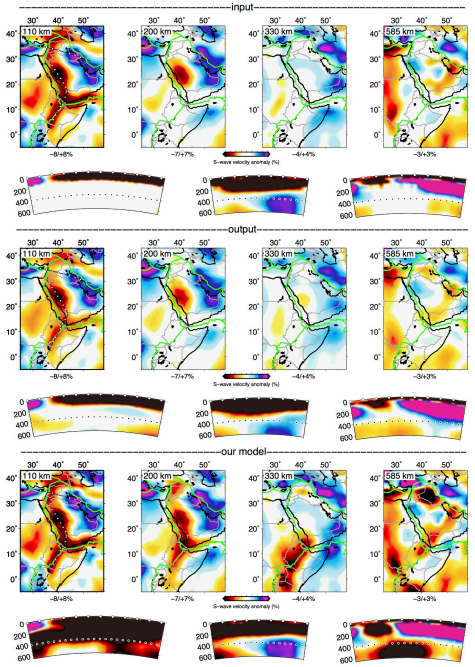
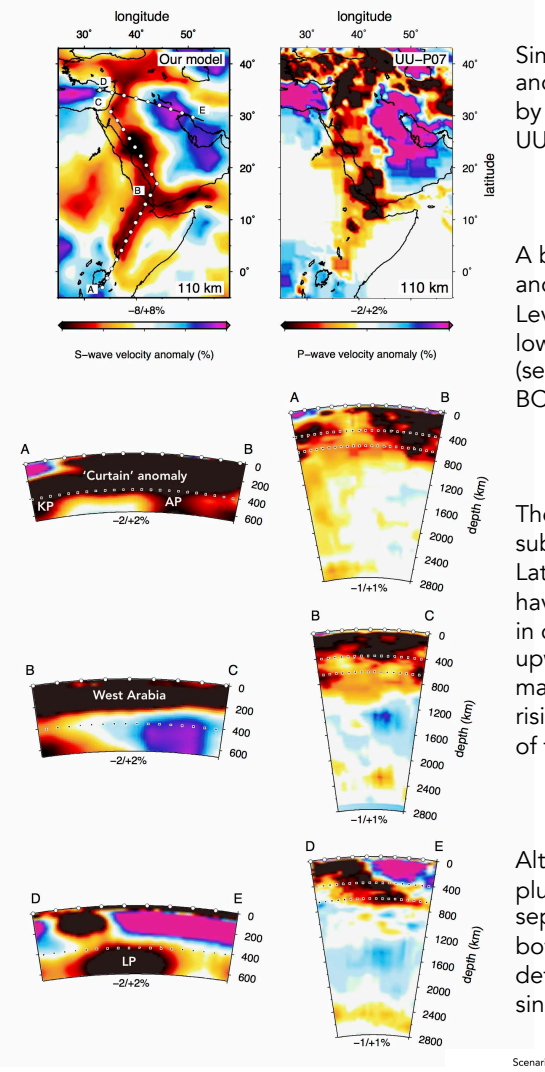


Figure 6. 'Structural' resolution test. The low-velocity anomalies below East Africa and below the Levant region are cut off in the input at depths ≥150 km.

6. Lower-mantle source?



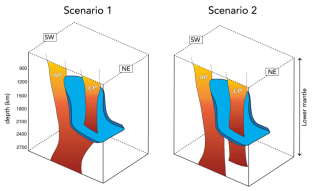
Similar low-velocity anomalies captured by the global model UU-P07.

A broad high-velocity anomaly cuts the Levant Plume at mid-lower mantle depths (see cross sections BC and DE).

The Arabian slab, subducted during Late Cretaceous may have broken and split in different upwellings the single mantle upwelling rising from the base of the lower mantle.

Alternatively, the two plumes are entirely separate upwellings, both perturbed and deflected by the sinking slab material

Figure 7. Top: Comparison of our tomographic model with the global P-wave model UU-P07 [*Amaru, 2007*]. Right: Two possible sceanrios, which reproduce the ancient Arabian slab crossing the two plumes.



7. Transition zone thickness

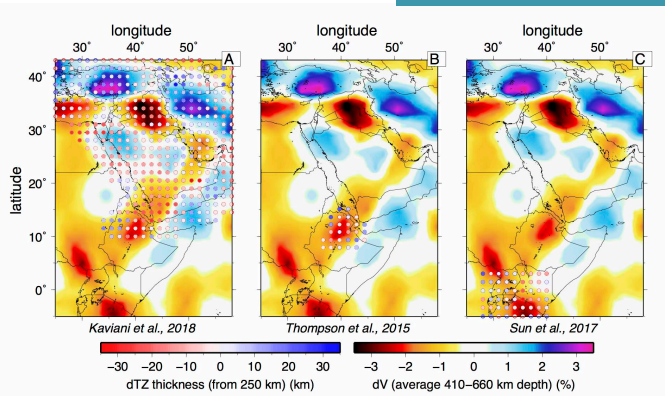


Figure 8. Comparison between the average velocity anomaly and the thickness of the transition zone from published receiver functions [*Kaviani et al., 2018; Thompson et al., 2015; Sun et al., 2017*].

The elevated temperatures in the TZ indicated by the low velocities where the three plumes rise through it are confirmed by receiver-function studies.

Differential arrival times of the P-to-S conversions indicate anomalously thin—and, thus, anomalously hot —TZ below Iraq, Afar, and Kenya.

DIAS Dublin Institute for Advanced Studies
cciviero@cp.dias.ie
#vEGU21
vEGU21: Gather Online | 19-30 April 2021

8. Global models

Overall match between the low-velocity anomalies at large scales.

The higher resolution provided by our new model allows us to resolve the structure with unprecedented detail.

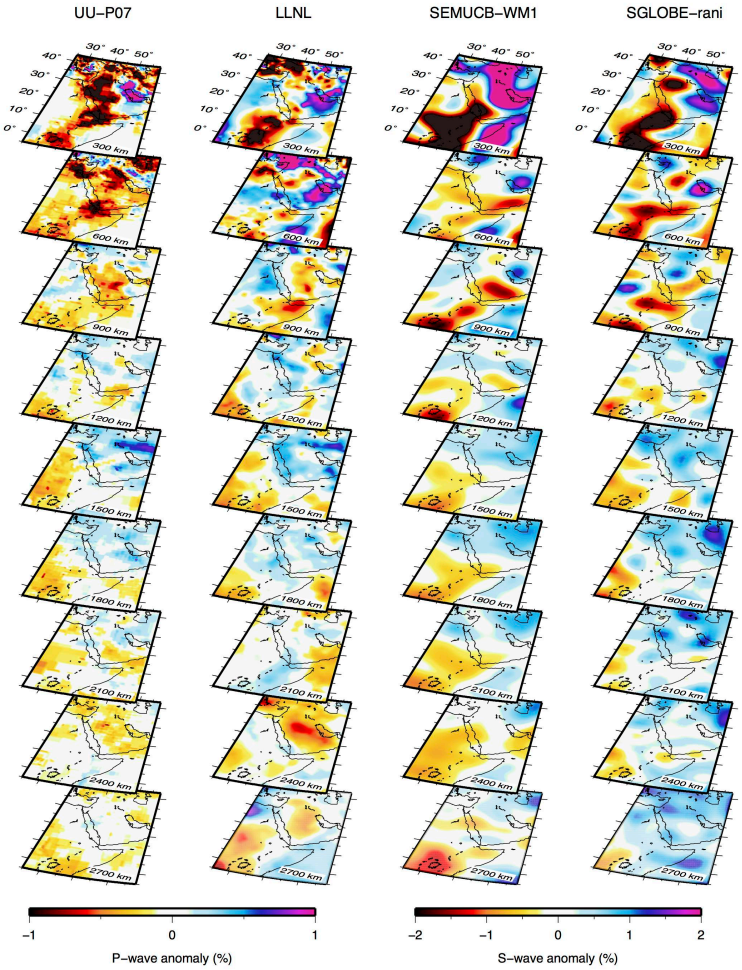


Figure 9. Global tomographic models through the whole mantle below the study region. Tomographic depth slices are shown for the following models: UU-P07 [*Amaru, 2007*]; LLNL [*Simmons et al., 2012*]; SEMUCB-WM1 [*French and Romanowicz, 2014*]; SGLOBE-rani [*Chang et al., 2015*].

9. Vote maps and cross sections

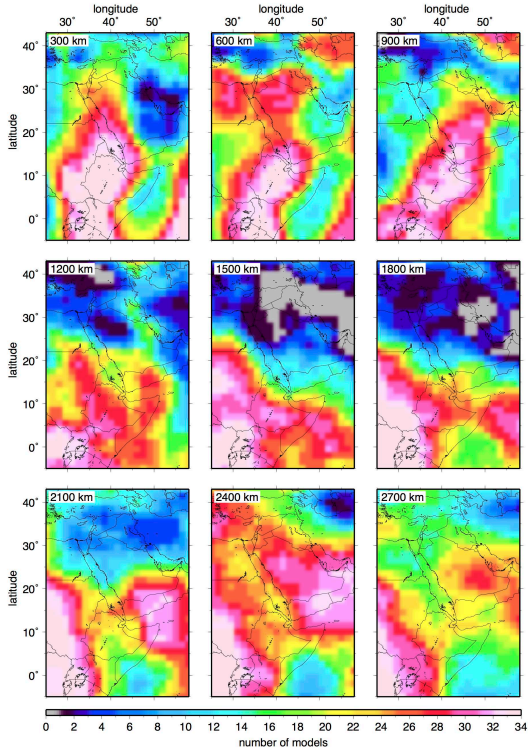


Figure 10. Low-velocity vote maps for 34 tomographic models (dv/v < 0). The voting maps are obtained stacking *P*- and *S*-wave models available in the *SubMachine* tomography web portal [*Hosseini et al. 2018*].

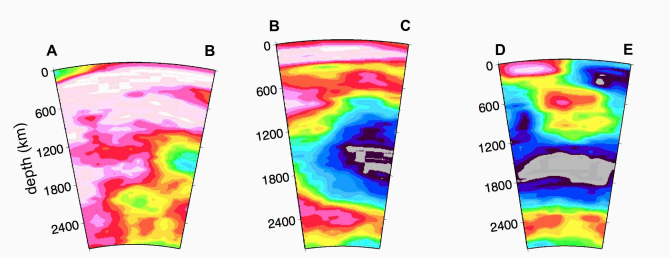


Figure 11. Low-velocity cross-sections for 34 tomographic models (dv/v < 0). The cross-sections are the same as those of our model.

dv/v < 0 (seismically slow areas)

A vote image is produced by stacking together N (where N≥1) P- and S-wave tomography models, in our case 34.

Maximum-vote region below East Africa, capturing well the shape and extent of the 'curtain-like' anomaly.

The low-velocity channel below Western Arabia is identified with a high-vote elongated area, which appears as a continuation of the low-velocity curtain below East Africa.

High level of consistency in assigning low velocities predominantly in two main clusters:

- under offshore Somalia and Arabia;
- beneath East and Central Africa.

High votes are observed below Iraq in agreement with our tomographic images, which show a strong low-velocity anomaly, interpreted as the tail of the Levant mantle plume.

cciviero@cp.dias.ie

10. Plate reconstruction

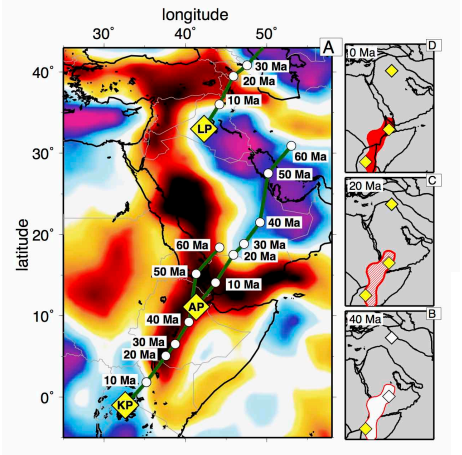
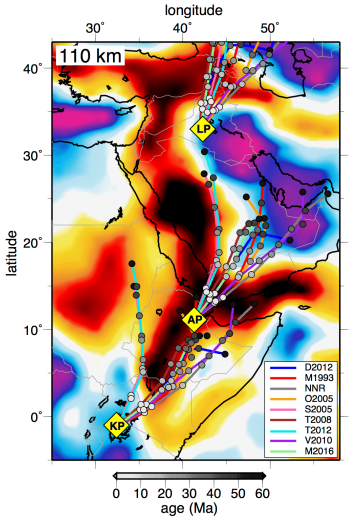


Figure 12. Predicted hotspot tracks. A) Tracks of the Afar plume (AP), Kenya plume (KP) and Levant plume (LP) relative to Arabian plate according to the reference frame of *Torsvik et al. [2019]*. The track is extended back to 60 Ma. White dots along tracks are in 10 Myr intervals. The three plumes are indicated with yellow diamonds.

Figure 13. Plume tracks at 0-60 Ma according to different plate-motion models. The different tracks show the variability of results depending on how the plate motion model was built. The dots are differently colored according to the age in Ma.



The Kenya Plume was below Ethiopia at 40-50 Ma and initiated the volcanism.

No old volcanism below Arabia associated with the Afar Plume > The Kenya Plume may have initiated volcanism in Ethiopia while the Afar plume was still rising in the lower mantle below the Arabian Platform.

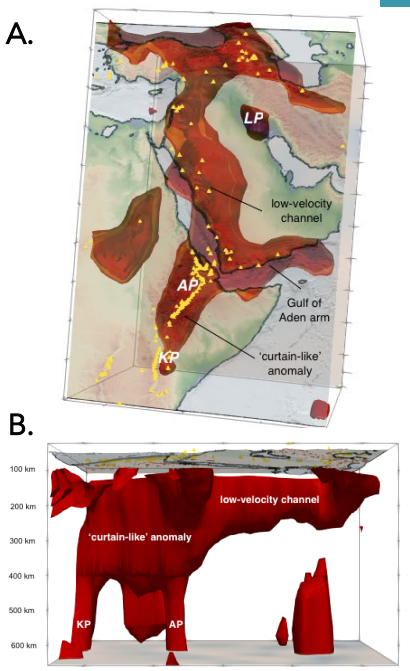
The passage over the Kenya Plume thinned the lithosphere, facilitating the flow of the material N-ward.

The curtain formed between the Kenya Plume in the south and the Afar Plume in the north.

Acknowledgements

This work is supported by the Science Foundation Ireland, the Geological Survey of Ireland, and the Marine Institute (grant 16/IA/4598).

11. Take-home message



- ✓ Intraplate volcanism in East Africa-Middle East fed by at least three deep upwellings, the Kenya, Afar and Levant Plumes forming a single living head.
- ✓ Hot material in the upper mantle flowing between the Kenya and Afar Plumes forming the 'curtain' beneath East Africa.
- ✓ Star-shaped non–convex plume heads may be more common than spherical plume heads.
- ✓ Complex feedback between the channeling of hot material in thinner-lithosphere areas, and the thinning of the lithosphere due to the arrival of the plume below the lithosphere.
- ✓ This mechanism of plume-continent dynamics can be occurring in many areas affected by continental riftingand ancient LIPs (e.g., NAIP, CAMP magmatism).

Figure 14. Three-dimensional view of three-pronged East Africa-Middle East plume head (A) and of the N-S profile showing the curtain between the Kenya and Afar Plumes (B). Low-velocity at -2% are plotted in the upper mantle.

References

1. N. L. Celli, L. Lebedev, A. J. Schaeffer, C. Gaina, *Nat. Commun.* **11**, 92 (2020).
2. S. S. Gao, K. H. Liu, M. G. Abdelsalam, *J. Geophys. Res. Solid Earth.* **115**, 1–15 (2010).
3. A. Kaviani, E. Sandvol, A. Moradi, G. Rümpker, Z. Tang, P. M. Mai, *J. Geophys. Res. Solid Earth.* **123**, 4886–4905 (2018).
4. D. A. Thompson, J. O. S. Hammond, J-M. Kendall, G. W. Stuart, G. Helffrich, D. Keir, A. Ayele, B. Goitom, *Geochem. Geophys. Geosyst.* **16**, 834–846 (2015).
5. M. Sun, K. H. Liu, X. Fu, S. S. Gao, *Geophys. Res. Lett.* **44**, 12116–12124 (2017).
6. M. L. Amaru, *Geol. Ultraiectina*. 274, 174 (2007).
7. N. A. Simmons, S. C. Myers, G. Johannesson, E. Matzel, *J. Geophys. Res. Solid Earth.* **117**, B10302 (2012).
8. S. W. French, B. A. Romanowicz, *Geophys. J. Int.* **199**, 1303–1327 (2014).
9. S. Chang, A. M. G. Ferreira, J. Ritsema, H. J. Heijst, J. H. Woodhouse, *J. Geophys. Res. Solid Earth.* **120**, 4278–4300 (2015).
10. K. Hosseini, K. J. Matthews, K. Sigloch, G. E. Shephard, M. Domeier, M. Tsekhmistrenko, 2018. Geochem. Geophys. Geosyst. **19**, 1464–1483 (2018).
11. T. H. Torsvik, B. Steinberger, G. E. Shephard, P. V. Doubrovine, C. Gaina, M. Domeier, C. P. Conrad, W. W. Sager, Geochem. Geophys. Geosyst. **20**, 3659–3689 (2019).